Available online at www.sciencedirect.com

SciVerse ScienceDirect

journal homepage: www.elsevier.com/locate/he

Synthesis and evaluation of $(La_{0.6}Sr_{0.4})(Co_{0.2}Fe_{0.8})O_3$ (LSCF)–$Y_{0.08}Zr_{0.92}O_{1.96}$ (YSZ)–$Gd_{0.1}Ce_{0.9}O_{2-\delta}$ (GDC) dual composite SOFC cathodes for high performance and durability

Hyun Jun Ko [a], *Jae-ha Myung* [a], *Ji-Hwan Lee* [a], *Sang-Hoon Hyun* [a,*], *Jong Shik Chung* [b]

[a] *School of Advanced Materials Science and Engineering, Yonsei University, Seoul 120-749, Republic of Korea*

[b] *Department of Chemical Engineering, Pohang University of Science and Technology, San 31, Hyoja-dong, Nam-ku, Pohang 790-784, Republic of Korea*

ARTICLE INFO

Article history:
Received 26 May 2012
Received in revised form
3 August 2012
Accepted 22 August 2012
Available online 13 September 2012

Keywords:
Solid oxide fuel cell
Composite cathode
Polymerizable complex method
$Y_{0.08}Zr_{0.92}O_{1.96}$ $Gd_{0.1}Ce_{0.9}O_{2-\delta}$
$(La_{0.6}Sr_{0.4})(Co_{0.2}Fe_{0.8})O_3$

ABSTRACT

This paper investigates a $(La_{0.6}Sr_{0.4})(Co_{0.2}Fe_{0.8})O_3$ (LSCF)–$Y_{0.16}Zr_{0.92}O_{1.96}$ (YSZ)–$Gd_{0.1}Ce_{0.9}O_{2-\delta}$ (GDC) dual composite cathode to achieve better cathodic performance compared to an LSM/GDC–YSZ dual composite cathode developed in previous research. To synthesize the structures of the LSCF/GDC–YSZ and LSCF/YSZ–GDC dual composite cathodes, nano-porous composite cathodes containing LSCF, YSZ, and GDC were prepared by a two-step polymerizable complex (PC) method which prevents the formation of YSZ–GDC solid solution. At 800 °C, the electrode polarization resistance of the LSCF/YSZ–GDC dual composite cathode showed to be significantly lower (0.075 Ω cm^2) compared to that of a commercial LSCF–GDC cathode (0.195 Ω cm^2), a synthesized LSCF/GDC–YSZ dual composite cathode (0.138 Ω cm^2), and an LSM/GDC–YSZ dual composite cathode (0.266 Ω cm^2) respectively. Moreover, the Ni–YSZ anode-supported single cell containing the LSCF/YSZ–GDC dual composite cathode achieved a maximum power density of 1.24 W/cm^2 and showed excellent durability without degradation under a load of 1.0 A/cm^2 over 570 h of operation at 800 °C.

1. Introduction

Solid oxide fuel cells (SOFCs) are a promising next generation power generation system due to their high energy efficiency and flexibility to utilize various fuels. Moreover, SOFCs can result in reduced CO_2 emissions compared to most currently available hydrocarbon fuel systems. Recently, much focus has been placed on the development of SOFCs which can achieve both high power density and long-term stability. Most SOFCs are still operated at temperatures of 800 °C or above to avoid large polarization losses, thermal mismatch, and interfacial diffusion [1–6]. To reduce the large polarization losses, LSM/GDC–YSZ dual composite cathodes have been introduced where the LSM and GDC nano-particles are both coated on the YSZ core particles which results in greater performance and durability, demonstrated in our previous research [5,7]. The main purpose of introducing dual composite cathodes is to create an ideal cathode microstructure which improves phase contiguity and interfacial coherence [5]. To achieve this sort of improved performance and a more durable cathode than the LSM/GDC–YSZ dual composite cathode, an LSCF–GDC based cathode has been introduced, because of its high catalytic

* *Corresponding author*. Tel.: +82 2 2123 2850; fax: +82 2 312 5375.
E-mail addresses: cprocess@yonsei.ac.kr, prohsh@yonsei.ac.kr (S.-H. Hyun).

0360-3199/$ – see front matter Copyright © 2012, Hydrogen Energy Publications, LLC. Published by Elsevier Ltd. All rights reserved.
http://dx.doi.org/10.1016/j.ijhydene.2012.08.099

activity. When using the LSCF–GDC cathode, it is generally inserted GDC interlayer between the LSCF–GDC cathode and YSZ electrolyte to prevent the formation of secondary phase such as $La_2Zr_2O_7$ and $SrZrO_3$. But even in this case, the GDC–YSZ solid solution, which decreases the ionic conductivity, can be formed by reaction between GDC interlayer and YSZ electrolyte and this may worsen the electrochemical performance of single cell. For that reason, it has been focused on the development of the single cell without using GDC barrier layer. Moreover, the YSZ material was added on the LSCF–GDC cathode to increase the interfacial coherence and interconnectivity with electrolyte.

In this study, two types of LSCF–YSZ–GDC dual composite cathodes have been evaluated to further improve the LSM/GDC–YSZ dual composite cathode performance. The two types of LSCF–YSZ–GDC dual composite cathode structures have been expressed as LSCF/YSZ–GDC and LSCF/GDC–YSZ, respectively; when LSCF and YSZ phases are placed on the GDC core particles, the structure is referred as LSCF/YSZ–GDC and vice versa for the other. A two-step polymerizable complex (PC) method based on polyesterification between citric acid (CA) and ethylene glycol (EG) was utilized for the synthesis of the nano-composite material, which also prevents the formation of GDC–YSZ solid solution among impregnation, co-precipitation, amorphous citrate, polymeric gel, glycine–nitrate process, citrate/sol–gel route and PC methods [9–13]. Moreover, YSZ electrolyte was used instead of GDC electrolyte due to the difficulty of securing the durability with GDC electrolyte under a reducing atmosphere at a low oxygen pressure [28]. The cathodic polarization resistance and the durability of the LSCF–YSZ–GDC dual composite cathode were examined and the fuel cell performances of Ni–YSZ anode-supported single cells containing the LSCF–YSZ–GDC cathode were evaluated.

2. Experimental

2.1. Synthesis of LSCF–YSZ–GDC dual composite powder

Fig. 1 shows the synthetic procedure of the LSCF–YSZ–GDC dual composite powder using a two-step polymerizable complex method [7]. Stoichiometric amounts of $LaN_3O_9{\bullet}6H_2O$ (Aldrich, 99.99%), SrN_2O_6 (Aldrich, 99+%), $Co(NO_3)_2{\bullet}6H_2O$ (Aldrich, 98+%), and $FeN_3O_9{\bullet}6H_2O$ (Aldrich, 98%) along with citric acid (Junsei Chemical Co., 99.5%) were dissolved in deionized water and subsequently, ethylene glycol (Ducksan Pure Chemical, 99.5%) and GDC (Rhodia) core particles were added. Upon heating at 120 °C, polyesterification between the metal ions (La, Sr, Co, and Fe), citric acid, and ethylene glycol occurred. The polymeric resin was transformed into LSCF conjugated on the GDC core particles after calcination at 800 °C. Experiments using LSCF–GDC as core particles proceeded with nitrate materials to synthesize the LSCF/YSZ–GDC dual composite materials. LSCF/GDC–YSZ dual composite materials were synthesized using the same synthesis procedure of the LSCF/YSZ–GDC dual composite materials. To identify the formation of crystalline phases without any secondary phases such as $La_2Zr_2O_7$, $SrZrO_3$, and a GDC–YSZ solid solution, the powders were characterized by X-ray diffraction (XRD, Ringaku). Then, the microstructure, composition distribution, and porosity of the composite powders were characterized by Scanning Electron Microscopy (SEM, FEI), Energy Dispersive Spectroscopy (EDS, FEI), and Archimedes method, respectively. Furthermore, an Electrophoretic Light scattering Spectrophotometer (ELS, Otsuka electronics) was utilized to confirm the existence of conjugated nano-sized particles on the core particles by observing the changes of the surface charge of the powder [14].

2.2. Electrical analysis and performance evaluation of LSCF–GDC–YSZ dual composite cathodes

To evaluate the cathodic performance of the composite cathodes, symmetric cells (cathode layer//YSZ electrolyte//cathode layer) were prepared using two different types of composite cathode: LSCF/GDC–YSZ dual composite and LSCF/YSZ–GDC dual composite cathodes. The composite cathodes were screen-printed on both sides of YSZ discs (sintered at 1400 °C for 3 h) and fired at 850 °C, 900 °C, and 950 °C. Electrochemical impedance measurements were performed on the symmetric cells using AC impedance spectroscopy (Solartron SI 1260/1287) and in the frequency range of 100 kHz–0.1 Hz with an applied AC voltage amplitude at 800 °C. Thermal cycle tests were completed by the schedule as proceeded in our earlier research [7,15–19].

Ni–YSZ anode-supported cells containing the LSCF/YSZ–GDC dual composite cathode were also fabricated to evaluate the fuel cell performance. NiO–YSZ anode supports (Ni:YSZ = 50:50 vol %) were formed by uni-axial pressing. Then, the anode supports were heated at 650 °C for 3 h to remove the pore former and were pre-sintered at 1200 °C for 3 h. A thin and dense YSZ electrolyte (6–7 μm) was dip-coated onto the anode support. One side of the support (YSZ//anode support//YSZ) was polished to eliminate the YSZ electrolyte after sintering at 1350 °C for 3 h. Finally, the LSCF/YSZ–GDC dual composite cathode was screen-printed on the top of the YSZ/anode support, followed by firing at 900 °C for 4 h. The fuel cell performance and long-term stability of the Ni–YSZ anode-supported unit cells were measured using hydrogen as a fuel and air as an oxidant at 800 °C and 650 °C.

3. Results and discussion

3.1. Characteristics of the LSCF–YSZ–GDC dual composite powder

To confirm the synthesis results and the formation of secondary phases, the peaks of the synthesized LSCF/YSZ–GDC and LSCF/GDC–YSZ particles were compared with commercial YSZ, GDC, and LSCF peaks. As seen in Fig. 2, only the primary phases including the LSCF perovskite, YSZ cubic, and GDC cubic phases were detected without formation of YSZ–GDC solid solution, $La_2Zr_2O_7$, and $SrZrO_3$. This demonstrates that the two-step PC method prevents the formation of secondary phases, as confirmed in previous results [7]. Fig. 3 (a) and (b) show the zeta potential values and electroosmotic stream plot (EOS plot) of the commercial GDC and synthesized

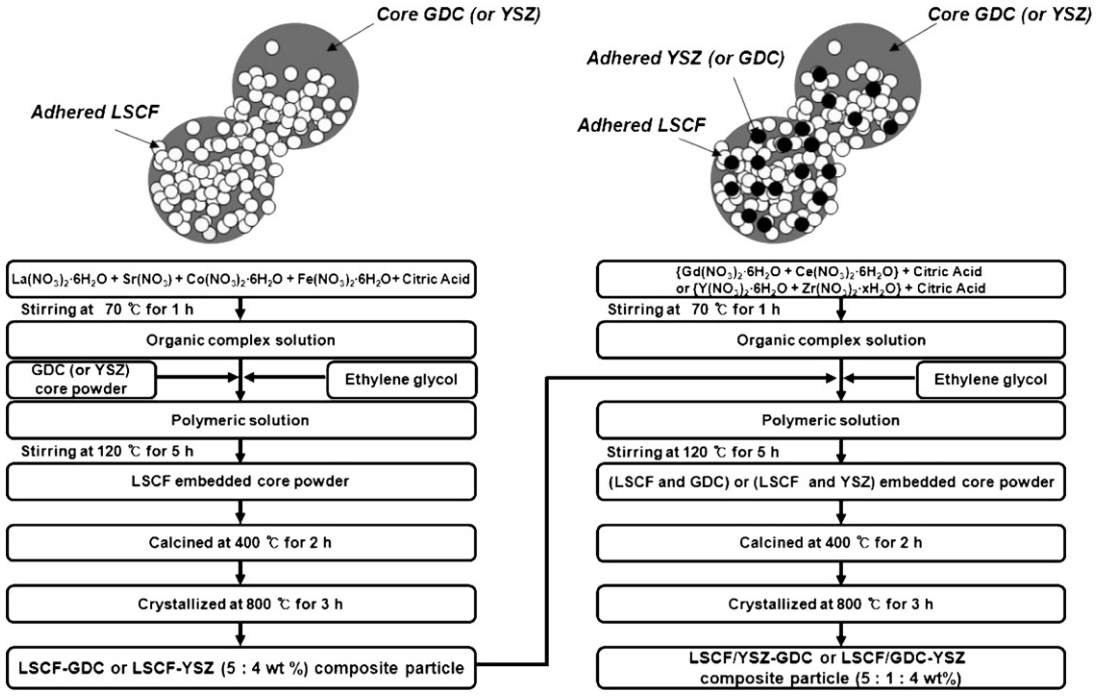

Fig. 1 – Ideal structures of nano-composite powders and flow charts of the synthesis processes of the LSCF/YSZ–GDC and LSCF/GDC–YSZ dual composite powders.

LSCF/YSZ–GDC dual composite particles. The existence of conjugated nano-particles on the GDC core particles can be confirmed from the surface charge difference between the commercial GDC core particles (29.56 mV) and the synthesized LSCF/YSZ–GDC dual composite particles (–6.67 mV). Moreover, the zeta potential levels of the LSCF/YSZ–GDC dual composite particles maintained parabolic shapes demonstrating that the coated particles were well dispersed on the core particles [14]. Even in the LSCF/GDC–YSZ dual composite particles, a similar phenomenon was observed, as seen in Fig. 3 (c) and (d). To prove that the conjugated nano-particles are LSCF and YSZ phases, SEM–EDX observations were made. As seen in Fig. 4, nano-sized LSCF and YSZ particles (15–20 nm) were thoroughly placed on the GDC core particles and the LSCF/YSZ–GDC dual composite particles existed as ~490 nm sized agglomerates.

3.2. *Performance evaluation of the LSCF–GDC–YSZ dual composite cathode*

The total interfacial polarization resistances of symmetric cells containing the LSCF/GDC–YSZ and LSCF/YSZ–GDC dual composite cathodes with respect to the cathode firing temperature are shown in Fig. 5. The electrode polarization resistance of the cathode is represented as half of the total interfacial polarization resistance of the symmetric cell, which is comprised of two symmetrical cathodes [20]. Hence, the electrode polarization resistances of the LSCF/YSZ–GDC dual composite cathodes fired at 850 °C, 900 °C, and 950 °C were 0.142 Ω cm^2, 0.075 Ω cm^2 and 0.115 Ω cm^2, respectively. Polarization resistances of 0.204 Ω cm^2 (850 °C), 0.138 Ω cm^2 (900 °C) and 0.172 Ω cm^2 (950 °C) were obtained for the LSCF/GDC–YSZ dual composite cathodes. Moreover, the commercial LSCF–GDC cathode fired at 1000 °C showed a polarization resistance of 0.195 Ω cm^2. Therefore, the LSCF/YSZ–GDC dual composite fired at 900 °C showed the lowest electrode polarization resistance (0.075 Ω cm^2) compared to the commercial LSCF–GDC cathode (0.195 Ω cm^2) and the LSCF/GDC–YSZ dual composite cathode (0.138 Ω cm^2). The LSCF/YSZ–GDC (surface area: 14.686 m^2/g) and LSCF/GDC–YSZ (surface area: 19.525 m^2/g) dual composite cathodes showed better performances than the commercial LSCF–GDC cathode due to the

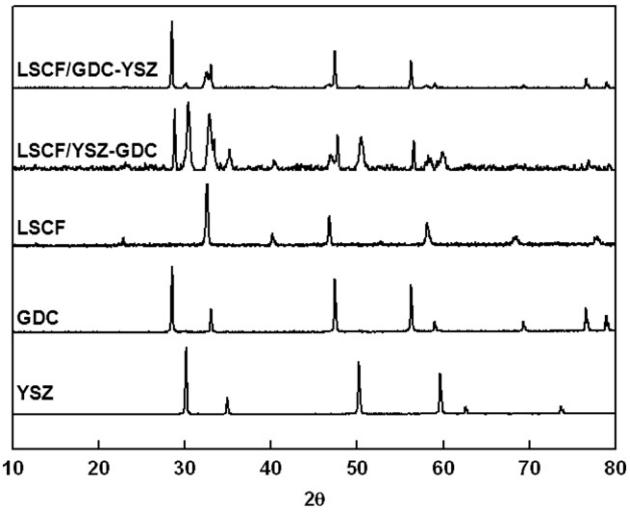

Fig. 2 – XRD patterns of commercial YSZ, GDC, LSCF, synthesized LSCF/YSZ–GDC, and LSCF/GDC–YSZ dual composite powders calcined at 800 °C.

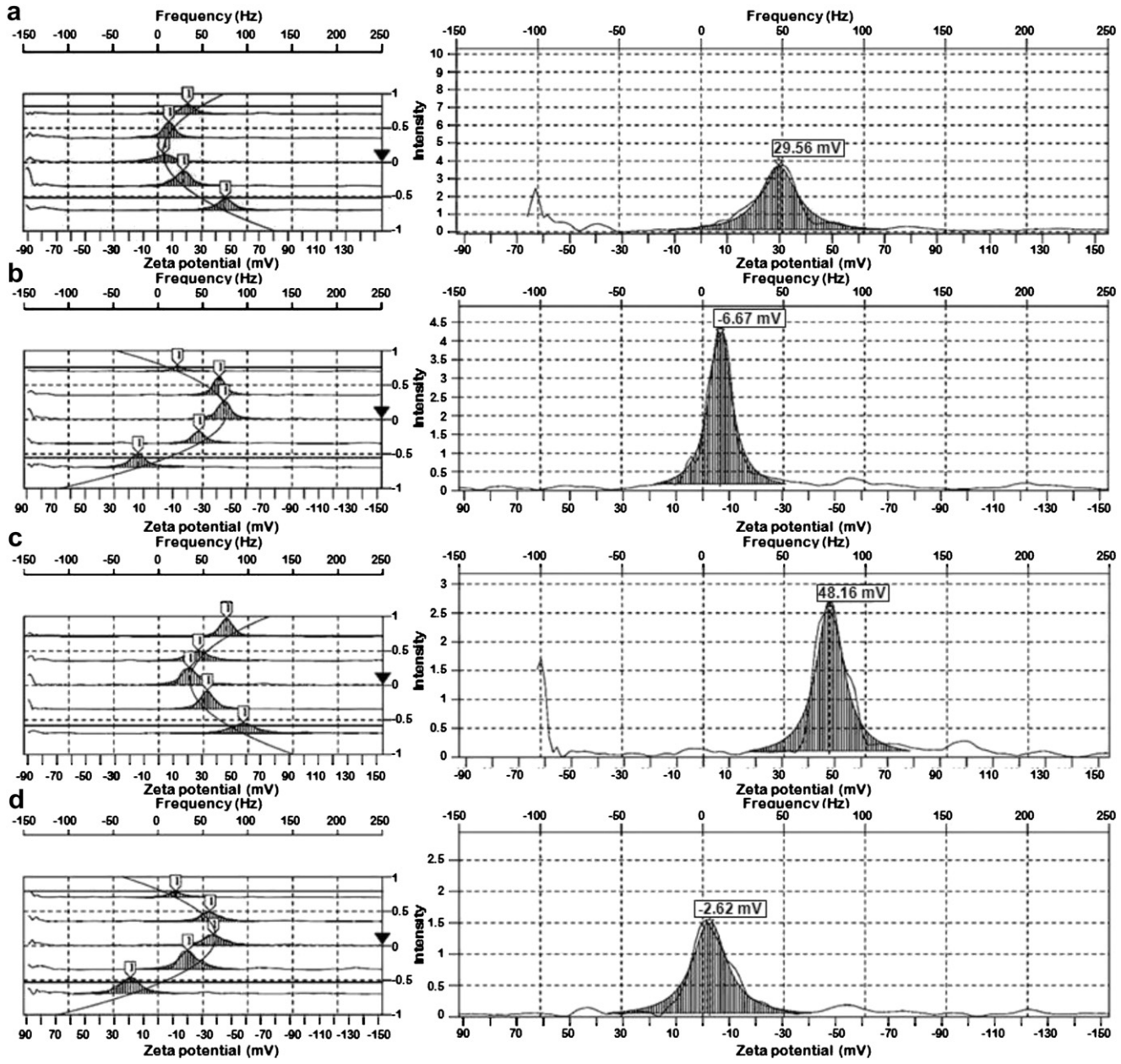

Fig. 3 – EOS plots and surface charges of (a) commercial GDC, (b) synthesized LSCF/YSZ–GDC dual composite powder, (c) commercial YSZ, and (d) synthesized LSCF/GDC–YSZ dual composite powder.

extension of the TPB reaction sites which can improve the electrochemical reaction [21–23]. It can be other reason that the high polarization resistance of the commercial LSCF–GDC cathode is low interfacial coherence with YSZ electrolyte because the GDC buffer layer was not inserted between cathode and electrolyte. In case of the LSCF/YSZ–GDC dual composite cathode, the YSZ nano-particles are coated on the cathode surface to improve the interfacial coherence with YSZ electrolyte. The large amounts of the GDC materials, which have a higher ionic conductivity than YSZ, are also composed within the cathode. Those are considered to be the reason that the LSCF/YSZ–GDC dual composite cathode demonstrated better performance than the LSCF/GDC–YSZ dual composite cathode. Moreover, the electrode polarization resistance of the LSCF/YSZ–GDC dual composite cathode was 75% lower than that of the LSM/GDC–YSZ dual composite cathode (0.266 Ω cm^2) because The LSCF materials do not only have a higher vacancy concentration and also have a better catalytic activity to oxygen reduction than LSM during the cathode reaction [8]. In this research, there are two important factors which determine the polarization resistance of the cathode. One factor is the porosity of the LSCF/YSZ–GDC dual composite cathode which depends on the firing temperature, as seen in Fig. 6. The cathode which was fired at 850 °C had a porosity of 44.3%. The high porosity can increases the electrode polarization resistance due to the low connectivity

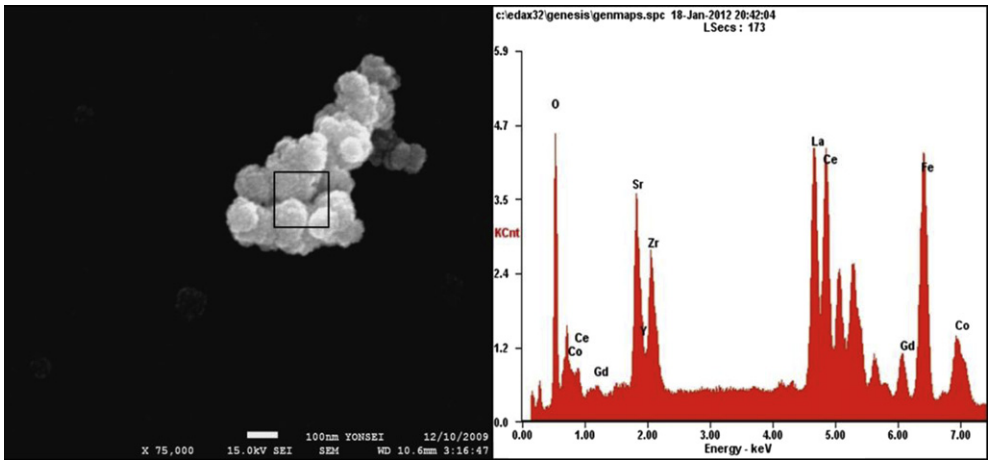

Fig. 4 – SEM–EDS data for the LSCF/YSZ–GDC dual composite powder.

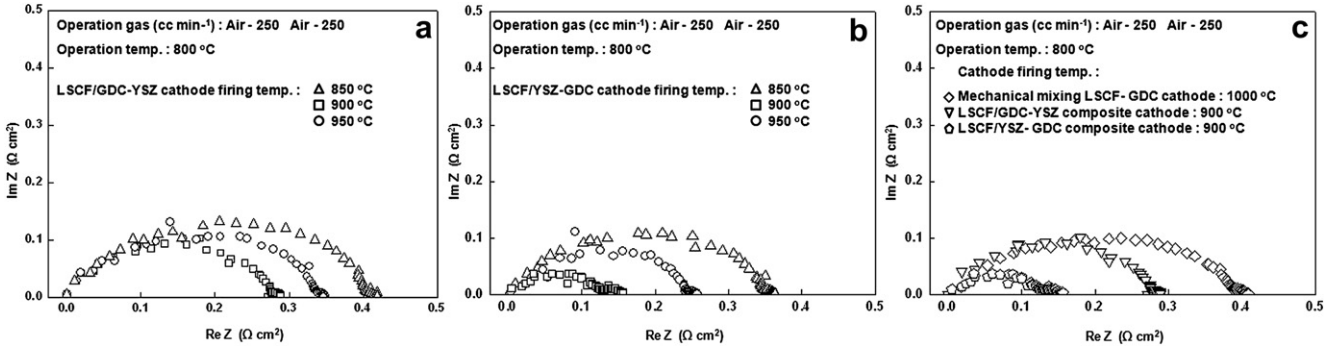

Fig. 5 – Electrode polarization resistances of the (a) LSCF/GDC–YSZ and (b) LSCF/YSZ–GDC dual composite cathodes with respect to the cathode firing temperature compared with a (c) commercial LSCF–GDC cathode.

between cathode particles. In contrast, when the cathode was fired at temperatures over 950 °C, exacerbation of the cathode pore structure which increases the mass transport resistance was caused by the over-sintered cathode particles. The other

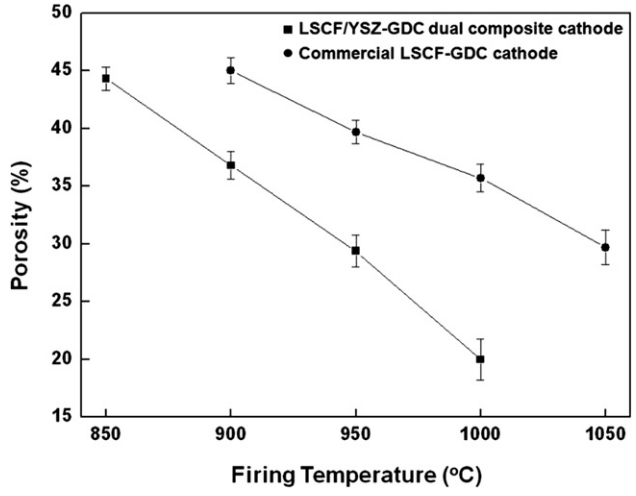

Fig. 6 – Porosities of LSCF/YSZ–GDC dual composite cathode and commercial LSCF–GDC cathode as a function of the firing temperature.

important factor is the formation of the secondary phase between LSCF and YSZ. According to other research, the secondary phases are generally formed at 1000 °C [24]. However, the formation temperature of the secondary phases can be reduced by of the high activity of the nano-sized cathode particles. To evaluate the reaction between LSCF and YSZ as a function of the firing temperature, nano-sized LSCF and YSZ particles synthesized by the PC method were mixed, fired and analyzed by XRD. Only the secondary phase of $SrZrO_3$ was detected when the firing temperature was over 850 °C, as seen in Fig. 7. However, a very small quantity of $La_2Zr_2O_7$ with respect to the total volume can be possibly existed, even though not detected by XRD. Those secondary phases are generally known that they can significantly undermine the electrochemical performance when they are spreading well between the LSCF and ionic phase. According to the previous research concerning the secondary phases of $La_2Zr_2O_7$ and $SrZrO_3$, $SrZrO_3$ do not have a serious effect on the electrochemical performance unlike $La_2Zr_2O_7$ [25]. Together, these results indicate that the increase of the cathodic polarization resistance is mostly caused by microstructural changes within the LSCF/YSZ–GDC dual composite cathode.

Thermal cycle testing was performed with the LSCF/YSZ–dual composite cathode and commercial LSCF–GDC

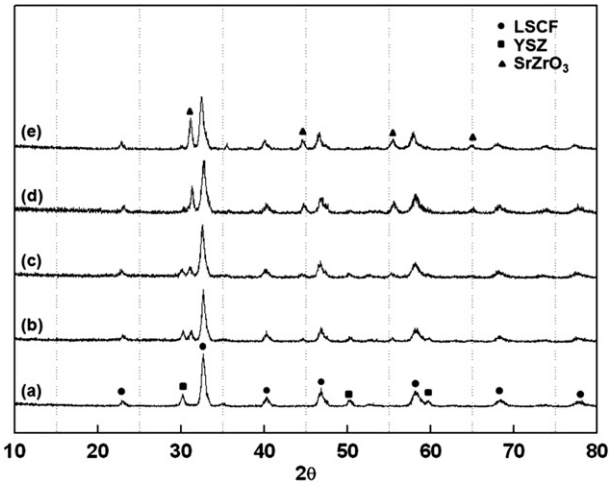

Fig. 7 – XRD patterns of the LSCF–YSZ composite powders as a function of the firing temperature: (a) as-calcined at 800 °C, (b) as-fired at 850 °C, (c) 900 °C, (d) 950 °C, and (e) 1000 °C.

cathode to confirm the cathode stability. After completing half of the 50 thermal cycle tests, the electrode polarization resistance of the commercial LSCF–GDC cathode increased by 138%. It is considered that the drastic reduction of the commercial LSCF–GDC cathode stability is caused by coarsening of the LSCF phase or the absence of the GDC buffer layer, which worsen the interconnectivity with the YSZ electrolyte [20,21,26,27]. However, for the LSCF/YSZ–GDC dual composite cathode, the electrode polarization resistance remained nearly constant after the 50 thermal cycle tests (Fig. 8). This result shows that the dual composite cathode maintains larger TPB sites and well established ionic/electronic conduction paths during the thermal cycle test.

Fig. 9 shows the fuel cell performance of the Ni–YSZ anode-supported single cells containing the LSCF/YSZ–GDC dual composite cathode. The maximum power densities were 0.5 W/cm^2 and 1.24 W/cm^2 at 650 °C and 800 °C, respectively,

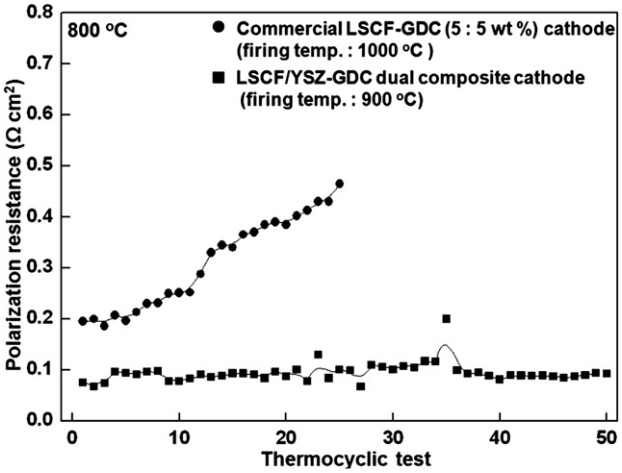

Fig. 8 – Thermocycle test data for the commercial LSCF–GDC cathode and LSCF/YSZ–GDC dual composite cathode.

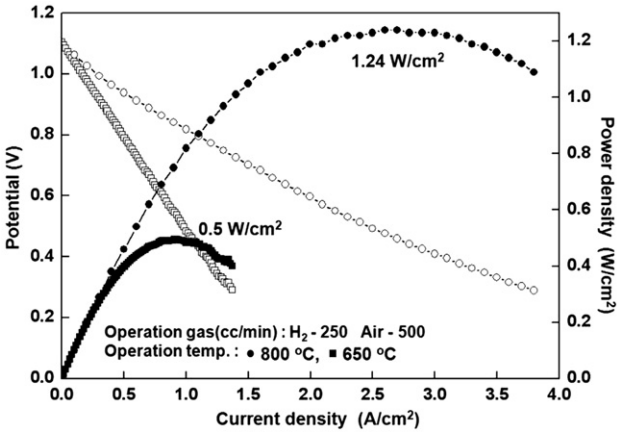

Fig. 9 – Electrochemical performance of a Ni–YSZ anode supported single cell containing the LSCF/YSZ–GDC dual composite cathode.

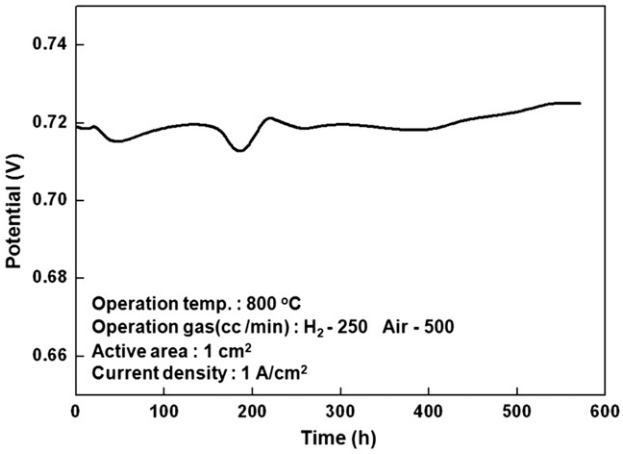

Fig. 10 – Long-term stability of a Ni–YSZ anode supported single cell containing the LSCF/YSZ–GDC dual composite cathode.

in reactive gases of hydrogen (250 cc/min) and air (500 cc/min). This represents a huge improvement of the fuel cell performance since the LSM/GDC–YSZ dual composite cathode was developed (maximum power density of 0.65 W/cm^2 at 800 °C) [7]. Furthermore, a durability test was performed under a static load of 1.0 A/cm^2 at 800 °C, as shown in Fig. 10. During 570 h of testing, the cell showed no degradation and maintained a voltage range of 0.719–0.725 V. This enhanced durability result is attributed to the microstructure stability, similar to the results of the thermal cycle testing.

4. Conclusion

LSCF/GDC–YSZ and LSCF/YSZ–GDC dual composite cathodes were investigated to enhance the electrochemical performance of the LSM/GDC–YSZ dual composite cathode which

was previously developed. The LSCF/GDC–YSZ and LSCF/YSZ–GDC dual composite cathode materials were successfully synthesized by a two-step polymerizable complex method which can prevent the formation of YSZ–GDC solid solution. In symmetrical half cell tests at 800 °C, the LSCF/YSZ–GDC dual composite cathode showed a lower electrode polarization resistance (0.075 Ω cm^2) than the commercial LSCF–GDC cathode (0.195 Ω cm^2) and the LSCF/GDC–YSZ dual composite cathode (0.138 Ω cm^2). Moreover, the cathodic performance of the LSCF/YSZ–GDC dual composite cathode was 75% better than that of the LSM/GDC–YSZ dual composite cathode (0.266 Ω cm^2) developed in previous research. This improvement of the cathodic performance is caused by using LSCF materials, which have high electrical conductivity and ionic conductivity, instead of LSM materials. After completion of the 50 thermal cycle tests, the electrode polarization resistance of the LSCF/YSZ–GDC dual composite cathode remained nearly constant. By contrast, the electrode polarization resistance of the commercial LSCF–GDC cathode increased by 138% after only 25 thermal cycles. Furthermore, a Ni–YSZ anode-supported single cell with the LSCF/YSZ–GDC dual composite cathode showed maximum power densities of 0.5 W/cm2 and 1.24 W/cm2 at 650 °C and 800 °C, respectively. At 800 °C, this single cell did not show any degradation over 500 h of operation under a load of 1.0 A/cm2.

Acknowledgments

This work was supported by a New & Renewable Energy grant of the Korea Institute of Energy Technology Evaluation and Planning (KETEP) funded by the Korean Ministry of Knowledge Economy (2009T100100344).

REFERENCES

[1] Ivers-Tiffée E, Weber A, Herbstritt D. Materials and technologies for SOFC-components. Journal of the European Ceramic Society 2001;21:1805–11.
[2] Mogensen M, Skaarup S. Kinetic and geometric aspects of solid oxide fuel cell electrodes. Solid State Ionics 1996;86-88: 1151–60.
[3] Ivers-Tiffée E, Weber A, Schmid K, Krebs V. Macroscale modeling of cathode formation in SOFC. Solid State Ionics 2004;174:223–32.
[4] Kuznecov M, Otschik P, Obenaus P, Eichler K, Schaffrath W. Diffusion controlled oxygen transport and stability at the perovskite/electrolyte interface. Solid State Ionics 2003;157: 371–8.
[5] Song HS, Lee S, Lee D, Kim H, Hyun SH, Kim J, et al. Functionally-graded composite cathodes for durable and high performance solid oxide fuel cells. Journal of Power Sources 2010;195:2628–32.
[6] Cao H, Deng Z, Li X, Yang J, Qin Y. Dynamic modeling of electrical characteristics of solid oxide fuel cells using fractional derivatives. International Journal of Hydrogen Energy 2010;35:1749–58.
[7] Ko H, Myung J-h, Hyun S-H, Chung J. Synthesis of LSM–YSZ–GDC dual composite SOFC cathodes for high-performance power-generation systems. Journal of Applied Electrochemistry 2012;42:209–15.
[8] Lee S, Song HS, Hyun SH, Kim J, Moon J. LSCF–SDC core–shell high-performance durable composite cathode. Journal of Power Sources 2010;195:118–23.
[9] Jiang SP, Leng YJ, Chan SH, Khor KA. Development of (La, Sr) MnO_3-based cathodes for intermediate temperature solid oxide fuel cells. Electrochemical and Solid State Letters 2003;6:A67–70.
[10] Nitadori T, Ichiki T, Misono M. Catalytic properties of perovskite-type mixed oxides (ABO3) consisting of rare earth and 3d transition metals. The roles of the A-and B-site ions. Bulletin of the Chemical Society of Japan 1988;61:621–6.
[11] Kremeni G, Nieto JML, Tascon JMD, Tejuca LG. Chemisorption and catalysis on $LaMO_3$ oxides. Journal of the Chemical Society, Faraday Transactions 1 1985;81:939–49.
[12] Taguchi H, Matsuda D, Nagao M, Shibahara H. Synthesis of $LaMnO_3$ using poly (acrylic acid). Journal of Materials Science Letters 1993;12:891–3.
[13] Kakihana M, Arima M, Yoshimura M, Ikeda N, Sugitani Y. Synthesis of high surface area $LaMnO_{3+}$ d by a polymerizable complex method. Journal of Alloys and Compounds 1999;283: 102–5.
[14] Kim J, Lee H, Kang H-J, Park T. The targeting of endothelial progenitor cells to a specific location within a microfluidic channel using magnetic nanoparticles. Biomedical Microdevices 2009;11:287–96.
[15] Kim Y-M, Kim-Lohsoontorn P, Baek S-W, Bae J. Electrochemical performance of unsintered $Ba_{0.5}Sr_{0.5}Co_{0.8}Fe_{0.2}O_{3-\delta}$, $La_{0.6}Sr_{0.4}Co_{0.8}Fe_{0.2}O_{3-\delta}$, and $La_{0.8}Sr_{0.2}MnO_{3-\delta}$ cathodes for metal-supported solid oxide fuel cells. International Journal of Hydrogen Energy 2011;36: 3138–46.
[16] Leng Y, Chan SH, Liu Q. Development of LSCF–GDC composite cathodes for low-temperature solid oxide fuel cells with thin film GDC electrolyte. International Journal of Hydrogen Energy 2008;33:3808–17.
[17] Yang J, Muroyama H, Matsui T, Eguchi K. A comparative study on polarization behavior of (La, Sr)MnO_3 and (La, Sr) CoO_3 cathodes for solid oxide fuel cells. International Journal of Hydrogen Energy 2010;35:10505–12.
[18] Yen-Pei F. $Sm_{0.5}Sr_{0.5}Co_{0.4}Ni_{0.6}O_{3-\delta}$–$Sm_{0.2}Ce_{0.8}O_{1.9}$ as a potential cathode for intermediate-temperature solid oxide fuel cells. International Journal of Hydrogen Energy 2010;35: 8663–9.
[19] Barbucci A, Paola Carpanese M, Viviani M, Vatistas N, Nicolella C. Morphology and electrochemical activity of SOFC composite cathodes: I. experimental analysis. Journal of Applied Electrochemistry 2009;39:513–21.
[20] Lee D, Jung I, Lee SO, Hyun SH, Jang JH, Moon J. Durable high-performance $Sm_{0.5}Sr_{0.5}CoO_3$–$Sm_{0.2}Ce_{0.8}O_{1.9}$ core-shell type composite cathodes for low temperature solid oxide fuel cells. International Journal of Hydrogen Energy 2011;36: 6875–81.
[21] Song HS, Hyun SH, Kim J, Lee H-W, Moon J. A nanocomposite material for highly durable solid oxide fuel cell cathodes. Journal of Materials Chemistry 2008;18:1087–92.
[22] Song HS, Lee S, Hyun SH, Kim J, Moon J. Compositional influence of LSM-YSZ composite cathodes on improved performance and durability of solid oxide fuel cells. Journal of Power Sources 2009;187:25–31.
[23] Kim SD, Moon H, Hyun SH, Moon J, Kim J, Lee HW. Nano-composite materials for high-performance and durability of solid oxide fuel cells. Journal of Power Sources 2006;163: 392–7.
[24] Kindermann L, Das D, Nickel H, Hilpert K. Chemical compatibility of the LaFeO3 base perovskites ($La_{0.6}Sr_{0.4}$) $zFe_{0.8}M_{0.2}O_{3-\delta}$ (z = 1, 0.9; M = Cr, Mn, Co, Ni) with yttria stabilized zirconia. Solid State Ionics 1996;89:215–20.

[25] Myung J-h, Ko HJ, Park H-G, Hwan M, Hyun S-H. Fabrication and characterization of planar-type SOFC unit cells using the tape-casting/lamination/co-firing method. International Journal of Hydrogen Energy 2012;37:498–504.
[26] Tanner CW, Fung KZ, Virkar AV. The effect of porous composite electrode structure on solid oxide fuel cell performance. Journal of the Electrochemical Society 1997;144:21.
[27] Adler S, Lane J, Steele B. Electrode kinetics of porous mixed-conducting oxygen electrodes. Journal of the Electrochemical Society 1996;143:3554.
[28] Ko HJ, Lee JJ, Hyun SH. Structural stability of the GDC electrolyte for low temperature SOFCs depending on fuels. Electrochemical and Solid State Letters 2010;13: B113–5.